ACS OMEGA

http://pubs.acs.org/journal/acsodf

Article

New Insights into the Role of Ligand-Binding Modes in GC-DNA Condensation through Thermodynamic and Spectroscopic Studies

Sakshi Gupta, Soumya Aggarwal, and Manoj Munde*

Cite This: *ACS Omega* 2023, 8, 4554−4565

Read Online

ACCESS | Metrics & More | Article Recommendations | Supporting Information

ABSTRACT: In biological systems, the unprompted assembly of DNA molecules by cationic ligands into condensed structures is ubiquitous. The ability of ligands to provoke DNA packaging is crucial to the molecular organization and functional control of DNA, yet their underlined physical roles have remained elusive. Here, we have examined the DNA condensation mechanism of four cationic ligands, including their primary DNA-binding modes through extensive biophysical studies. We observed contrasting changes for these ligands binding to poly[dGdC]:poly[dGdC] (GC-DNA) and poly[dAdT]:poly[dAdT] (AT-DNA). Based on a CD spectroscopic study, it was confirmed that only GC-DNA undergoes B- to Ψ-type DNA transformation in the presence of ligands. In the fluorescence displacement assay (FDA), the ability of ligands to displace GC-DNA-bound EtBr follows the order: protamine^{21+} > cohex^{3+} > Ni^{2+} > spermine^{4+}, which indicates that there is no direct correlation between the ligand charge and its ability to displace the drug from the DNA, indicating that GC-DNA condensation is not just influenced by electrostatic interaction but ligand-specific interactions may also have played a crucial role. Furthermore, the detailed ITC-binding studies suggested that DNA−ligand interactions are generally driven by unfavorable enthalpy and favorable entropy. The correlations from various studies insinuate that cationic ligands show major groove binding as one of the preferred binding modes during GC-DNA condensation.

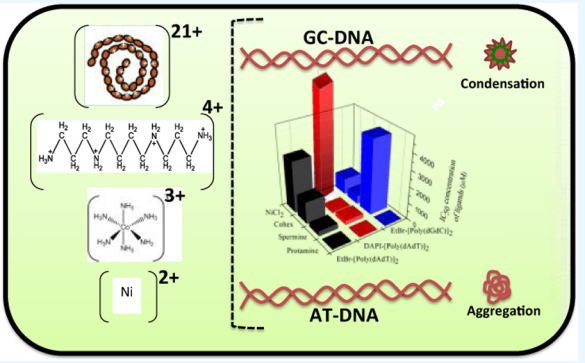

INTRODUCTION

DNA condensation is the phenomenon in which long DNA fragments experience compaction and aggregate into ordered, highly condensed states. Mounting evidence suggests that cells use DNA condensation as a mechanism to protect genetic material and regulate gene expression.[1] In the living organism, genomic DNA is a large, negatively charged, and quite rigid polymer that experiences huge compaction to fit in the few available spaces inside the cell.[2] In vivo DNA condensation is achieved by cationic proteins and polyamines.[3−9] It can also be achieved in vitro using neutral molecules such as alcohols, polyols, or charged ligands such as lipids, synthetic polymers, and peptides.[5,10−13] In the presence of these condensing agents, the collapse of the DNA occurs from its stretched coiled conformation to highly ordered nanosized particles. Apart from understanding the fundamental mechanism of DNA condensation, this topic has also garnered attention because of its applications in gene therapy and nanotechnology.[14]

Based on numerous earlier reports, several factors are known to affect DNA condensation such as the type of condensing agent, the concentration of salt, solvent dielectric constant, temperature, pH, as well as the concentration, length, and sequence of the DNA.[15] Apart from this, DNA−DNA and DNA−solvent interactions also contribute to condensation. A possible role of the intrinsic properties of DNA, such as its bendability and length, has also been discussed. However, these experimental approaches precluded the determination of the probable binding modes of cationic ligands within the DNA condensates.

Until now, the most conventional view with respect to DNA condensation has been based on an electrostatic model, which says that the collapse of the DNA occurs following an adequate amount of neutralization of negative charges on DNA by cationic ligands through electrostatic interactions.[3,16,17] Recently, studies have suggested a sequence dependence of DNA condensation, involving an important role for ligand-specific interactions.[6] However, more elaborative findings using a variety of cations and pure AT/GC sequences are necessary to reach a strong conclusion. In view of this, here, we have selected chemically diverse condensing agents such as protamine^{21+}, spermine^{4+}, $[Co(NH_3)_6]^{3+}$ (cobalt hexamine or cohex), and Ni^{2+} (nickel chloride) as shown in Figure 1. Protamine is known to bind DNA and produce a highly

Received: March 15, 2022
Accepted: September 20, 2022
Published: January 24, 2023

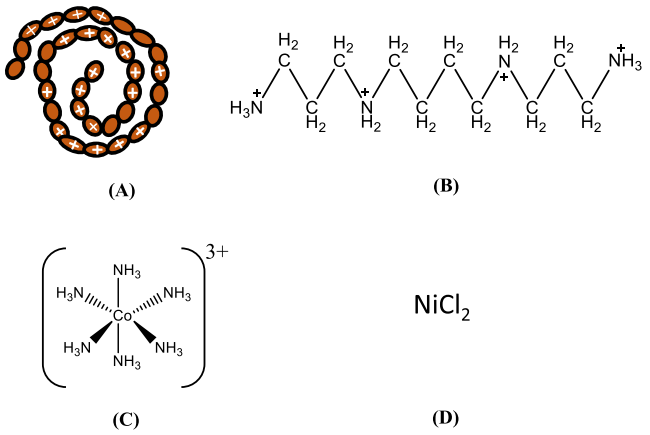

Figure 1. Chemical composition of (A) protamine (made up of a total of 33 amino acids of which 21 are Arg residues), (B) spermine, (C) cohex, and (D) $NiCl_2$.

condensed form of DNA within the sperm cell that inactivates the sperm genome.[18] Interestingly, protamine was found to preferably condense GC-DNA,[6] the exact mechanism of which is still unknown. Spermine demonstrated mixed binding modes in DNA condensation.[19] In fact, an extensive study of spermine derivatives also indicated the vital role of its diverse chemical structures in DNA condensation. Given the mixed outcomes, the precise binding mode of spermine responsible for DNA condensation remains unclear. Similarly, the role of the ligand charge in DNA condensation was truly challenged by cohex. It was observed that cohex has a similar charge to spermidine but a much greater DNA condensing capacity than the latter.[20] Besides, even though there is general agreement that a minimum of +3 cationic charge is essential for DNA condensation, divalent Ni^{2+} was found to condense DNA successfully.[21] Ni^{2+} ion has very fascinating properties (compared to other dications); for example, it shows a much higher specificity for the nitrogen of DNA bases.[22] This kind of knowledge implies that factors other than electrostatic interaction may also play an important role in DNA condensation; however, its systematic probing through qualitative as well as quantitative means is essential.

In view of this, the following questions are being raised: (i) DNA has several potential ligand-binding sites (groove, intercalation, and phosphate), which one of these would play a dominant role for a particular ligand and what are the driving (thermodynamic) forces behind it? (ii) Why are the DNA condensing strengths of cationic agents diverse, and why a proper correlation could not be established between the condensing ability and their chemical structure/charge/size? Such fundamental knowledge is crucial as it can provide inputs concerning the mechanism of DNA condensation and further into the development of gene therapeutics. Since it is highly difficult to obtain structural information of condensed DNA by X-ray crystallography, evaluating the ligand-binding mode using a combination of various experimental biophysical techniques seems to be the best possible way. Here, with the help of GC-rich and AT-rich polymeric DNA sequences and a variety of chemically diverse cationic ligands, we have tried to explore new insights into the process of DNA condensation.

MATERIALS AND METHODS

Poly[dGdC]:poly[dGdC] (GC-DNA) and poly[dAdT]:poly-[dAdT] (AT-DNA), protamine sulfate salt (from salmon), spermine, ethidium bromide (EtBr), cobalt hexamine (cohex), and 4′,6-diamidino-2-phenylindole dihydrochloride (DAPI) were bought from Sigma-Aldrich Co. and used without additional purification. Nickel(II) chloride was procured from Alfa Aesar. The approximate average length of base pairs is 800 in both GC- and AT-DNA. The concentrations of DNA solution were determined in the base pair (bp) by recording absorbance at 260 nm using molar extinction coefficients, ε_{256} = 16800 and ε_{260} = 13200 bpM^{-1} cm^{-1} for GC-DNA and AT-DNA, respectively.[23] To check whether the DNA is free of protein, the purity of DNA was calculated at the absorbance ratio of A_{260}/A_{280} nm. The value was in the range of 1.8−1.9, which directed that the DNA is pure and free of proteins.[24] The stock concentrations of DAPI and EtBr were prepared at 1 mM in HPLC water. Furthermore, 10 mM stock solutions were prepared for protamine, nickel chloride, spermine, and cohex using 10 mM HEPES buffer at pH 7.4.

Circular Dichroism. CD experiments were carried out under nitrogen using the Chirascan Applied Photophysics spectropolarimeter. Quartz cuvettes with a path length of 3 mm were used, and experiments were conducted at 25 °C. Samples were prepared by using constant (50 μM/bp) concentrations of GC-DNA and AT-DNA, whereas the concentration of ligand was variable: protamine (0−6 μM), spermine (100 μM to 20 mM), Ni^{2+} (100 μM to 8 mM), and cohex (50 μM to 3 mM) using 10 mM HEPES buffer at pH 7.4 containing 100 mM NaF. Samples were scanned in the wavelength range of 220−300 nm with a scan speed of 75 nm/min. Five runs with an approximate scan time of 11 min per scan were performed and averaged.

Gel Electrophoresis. The samples were prepared in 10 mM HEPES buffer and 100 mM NaCl by mixing GC-DNA (∼20 μM) with different concentrations of ligands, $NiCl_2$ (0−10 mM), spermine (0−2.0 mM), protamine (0−2 μM), and cohex (0−1 mM). 0.5% agarose gel was prepared to contain 0.5 μg/mL of EtBr for DNA staining during the run. To get the best results, all the prepared samples were incubated for 20 min at 4 °C, and in the case of protamine and cohex, the samples were centrifuged for 20 min at 14,000 rpm. ImageJ software was used to process gel images.

Isothermal Titration Calorimetry. ITC experiments were performed on the MicroCal iTC_{200} system at a 20 °C temperature, the detailed information of which is published elsewhere.[25−27] Experiments were conducted by titrating the ligand into 100 μM/bp of DNA. Control experiments were performed to ignore the heat released when the ligand is titrated into the buffer. The entire data was fitted using one set of site models or two sets of site models available in the Origin software. The fitting for the binding of cohex to GC-DNA (Figure 6D,H) was complex and done in two phases, where independent regression analyses for each set were carried out, and the parameters were recorded for the best fit. First, 7−11 data points were deleted from the binding isotherm, which was then fitted using a single set of the binding model. Next, the fitting was done for the second peak of the isotherm using a two-set-binding site model, where points 1−6 were deleted which belonged to phase 1. Thermodynamic parameters, that is, stoichiometry (N), binding constant (K_A), and enthalpy change (ΔH) were obtained as shown in Table 1. Using K_A and ΔH, the Gibbs free energy change ($\Delta G = -RT \ln K_A$) and entropy change ($\Delta G = \Delta H - T\Delta S$) can also be calculated.

UV Spectroscopy Measurements. The absorbance of each of the fixed concentrations of DNA samples (GC-DNA

https://doi.org/10.1021/acsomega.2c01557
ACS Omega 2023, 8, 4554−4565

Table 1. Thermodynamic Parameters for Binding of Ligands with GC- and AT-DNA[a]

system	N_1	$^*K_{A1}$ (M^{-1})	ΔH_1 (kcal/mol)	$^*T\Delta S_1$ (kcal/mol)	$^*\Delta G_1$ (kcal/mol)	N_2	$^*K_{A2}$ (M^{-1})	ΔH_2 (kcal/mol)	$^*T\Delta S_2$ (kcal/mol)	$^*\Delta G_2$ (kcal/mol)
					Spermine					
GC-DNA	0.3 ± 0.04	$1.0 \times 10^5 \pm 1.5 \times 10^4$	2.1 ± 0.5	9.4 ± 1.5	−7.3 + 1.3	0.9 ± 1.4	$8.0 \times 10^3 \pm 1.5 \times 10^3$	−1.8 ± 1.0	3.4 ± 0.5	−5.3 ± 0.7
AT-DNA	0.2 ± 0.01	$1.0 \times 10^6 \pm 2.6 \times 10^5$	1.1 ± 0.07	9.3 ± 1.1	−8.2 ± 1.7	0.16 ± 0.07	$1.0 \times 10^5 \pm 0.8 \times 10^4$	−0.15 ± 0.17	6.7 ± 1.1	−6.8 ± 0.9
					Protamine					
GC-DNA	0.02 ± 0.005	$3.2 \times 10^5 \pm 0.3 \times 10^5$	5.3 ± 1.8	12.7 ± 1.4	−7.5 ± 1.4					
AT-DNA	data could not be fitted									
					$NiCl_2$					
GC-DNA	0.8 ± 0.02	$2.3 \times 10^5 \pm 7.0 \times 10^4$	−1.1 ± 0.05	6.2 ± 0.8	−7.3 ± 1.5					
AT-DNA		$5.4 \times 10^4 \pm 0.6 \times 10^4$	−0.6 ± 0.2	5.8 ± 0.5	−6.4 ± 0.9					
					cohex					
[b]GC-DNA	0.24 ± 0.1	$1.5 \times 10^5 \pm 7.6 \times 10^4$	1.0 ± 0.3	8.1 ± 1.5	−7.1 ± 1.6	0.2 ± 0.03	$1.0 \times 10^7 \pm 5.5 \times 10^6$	0.5 ± 0.1	10.1 ± 1.9	−9.5 ± 1.9
[b]AT-DNA	0.55 ± 0.2	$2.1 \times 10^4 \pm 9.6 \times 10^3$	1.3 ± 0.4	7.2 ± 1.7	−5.9 ± 1.5	0.2 ± 0.04	$3.0 \times 10^6 \pm 0.7 \times 10^5$	−1.6 ± 0.3	7.2 ± 1.5	−8.8 ± 1.5

[a]Binding experiments were performed at 25 °C in phosphate buffer. [b]In the case of cohex, errors for N, ΔH, K_A, ΔG, N, and $T\Delta S$ are on a higher side due to the larger uncertainty in fitting the complex-binding curve.

and AT-DNA) was scanned from 200 to 400 nm in the Cary 100 UV−vis spectrophotometer by varying the protamine, spermine, Ni^{2+}, and cohex concentration. DNA−ligand samples (10 mM HEPES buffer, pH 7.4, 100 mM NaCl) were made in aliquots and incubated for 2 h at 4 °C. After incubation, the aliquots were centrifuged at 60,000 rpm for 10 min. To compare the amount of condensed DNA in the presence of various ligands, the absorbance values at 260 nm were normalized and plotted. In the time-dependent measurements, the effect of each of the DNA condensates was monitored separately. In the melting study, the absorbance change for each DNA in the absence and presence of ligand over a temperature range of 25−90 °C was recorded at 260 nm. All the melting studies were done at a constant concentration of 50 μM of DNA complexed with a ligand.

Fluorescence Displacement Assay. FDA was performed using a Cary Eclipse fluorescence spectrophotometer. Experiments were carried out at room temperature using a quartz cuvette of 1 cm path length with a scanning speed of 60 nm/min. The DNA concentration was fixed at 50 μM/bp. The saturated DNA−drug complex was prepared using 0.5 and 0.25 drug/DNA bp^{-1} ratios for EtBr and DAPI, respectively. The DNA−drug complex was titrated with varying concentrations of the ligand (protamine, spermine, Ni^{2+}, and cohex) from its lower to higher concentration. Fluorescence emission was recorded in the range of 500−700 nm by exciting EtBr at 480 nm and DAPI at 375 nm. The fluorescence intensities at the maximum wavelength were plotted against drug concentration, and the mid point of transition was used as the IC_{50} value.

RESULTS

Ligand-Induced Conformational Changes in DNA. CD is certainly the most prevalent technique for investigating the conformational modifications in the DNA helix after ligand binding. Figure 2 shows the effects of the addition of increasing amounts of four cationic ligands on the conformation of GC- and AT-DNA. Free GC-DNA displays a single positive peak at 274 nm and a negative peak at 254 nm, indicating the B-form of DNA.[7] Upon addition of spermine, no major shifting of CD bands was observed (Figure 2A), suggesting that spermine binds weakly to the GC sequence, which is in support of the previous studies;[28] however, there was a broadening of the peak around 274 nm. Notably, when protamine was titrated into GC-DNA, there was a reduction of intensity at 274 nm and a huge red-shift (275−295 nm) in wavelength (Figure 2B), followed by the broadening and flattening of the peak. Similar results were observed for Ni^{2+} and cohex (Figure 2C,D). Here, the red shifting and broadening of the spectrum induced by these cations has characteristics similar to the spectrum observed in the case of polymer-induced condensation (psi).[7]

In Figure 2E, AT-DNA shows a CD spectrum with a single positive peak at 262 nm, a weak shoulder peak at 280 nm, and a negative peak at 247 nm.[29] In the presence of spermine, there was a moderate decrease in the intensity, suggesting an alteration in the conformation of AT-DNA. Similarly, upon the addition of protamine (Figure 2F), there was an abrupt reduction in the DNA intensity, and at 100 μM, the DNA signal showed negative ellipticity with a slight blue shift from 275 to 265 nm. The CD patterns in 2E and 2F do not match with the ones observed in Figure 2A−D, and the constant decrease in the intensity here strongly suggests the formation of aggregates of DNA.[30] On the contrary, the binding of Ni^{2+}

https://doi.org/10.1021/acsomega.2c01557
ACS Omega 2023, 8, 4554−4565

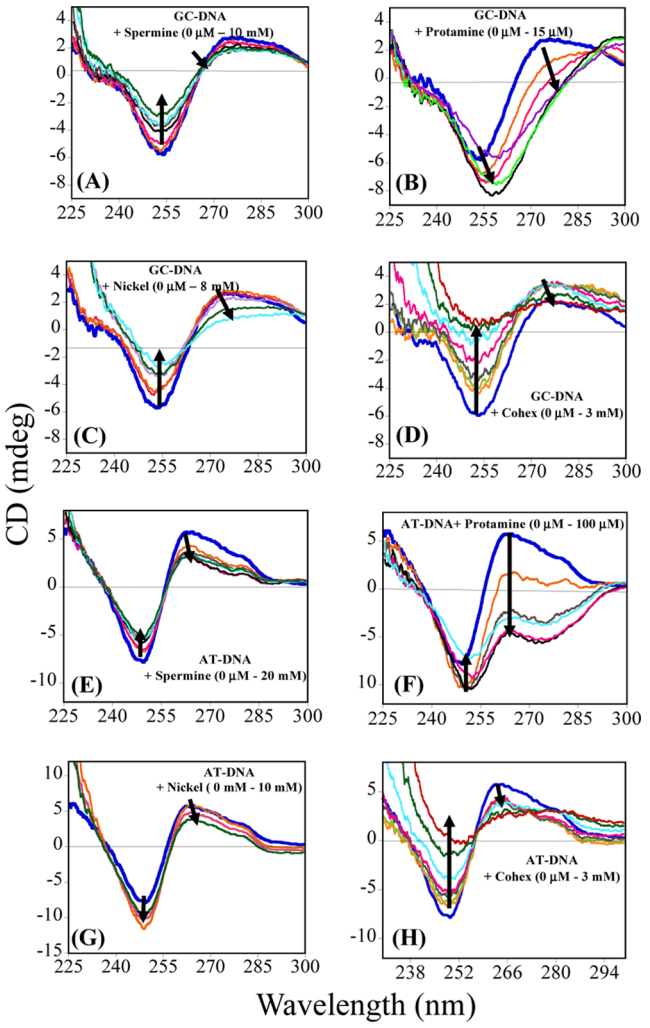

Figure 2. CD spectra of GC-DNA in the presence of (A) spermine (100 μM to 10 mM), (B) protamine (2−15 μM), (C) Ni^{2+} (100 μM to 8 mM), and (D) cohex (50 μM to 3 mM) and of AT-DNA in the presence of (E) spermine (500 μM to 20 mM), (F) protamine (8−100 μM), (G) Ni^{2+} (2−10 mM), and (H) cohex (50 μM−3 mM). The concentration of each DNA was 50 μM in base pairs. Melting profiles of GC- and AT-DNA with condensing ligands.

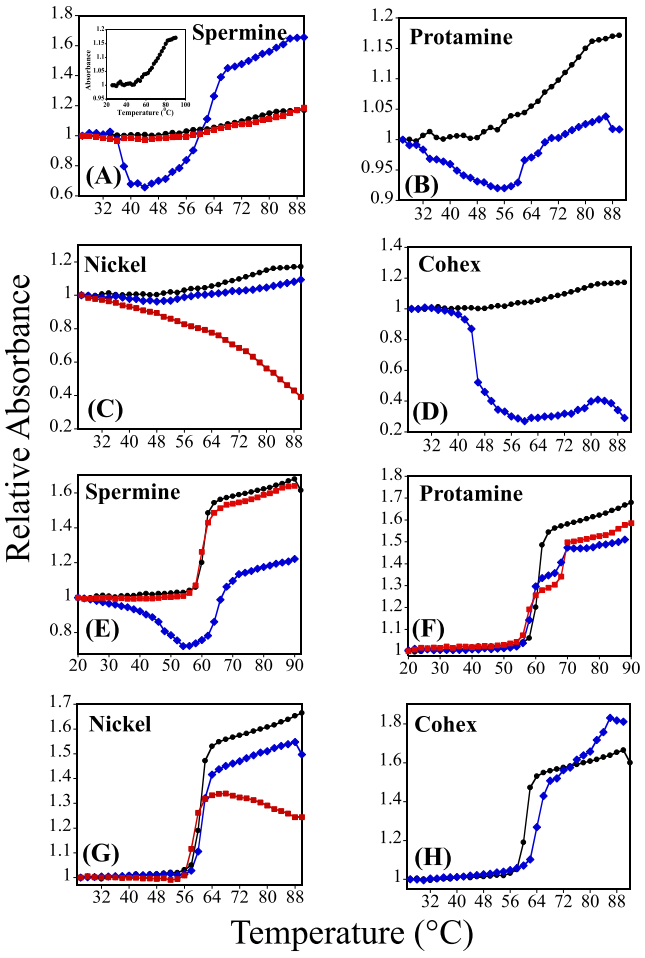

Figure 3. Melting profiles of GC-DNA in the presence of (A) spermine at 0 (●), 1 (■), and 4 mM (♦); in the inset, the enlarged spectrum of free DNA (in the absence of ligand); (B) protamine at 0 (●) and 2 μM (♦); (C) Ni^{2+} at 0 (●), 1 (■), and 2 mM (♦); and (D) cohex at 0 (●) and 1 mM (♦). AT-DNA in the presence of © spermine at 0 (●), 1 mM (♦), and 4 mM (■). (F) protamine at 0 (●), 1 μM (♦), and 4 μM (■). (G) Ni^{2+} at 0 (♦), 2 (■), and 4 mM (♦) and (H) cohex at 0 (●) and 1 mM (♦). The concentration of each DNA was 25 μM in base pairs.

(Figure 2G) to AT-DNA resulted in only a slight decrease in the CD spectrum, suggesting its lower binding capacity. In Figure 2H, cohex induces a small change in the intensity, suggesting that cohex is able to induce conformational alteration in AT-DNA, although of lower strength compared to protamine.

The effects of the condensing ligands on the thermal stability of the GC- and AT-DNA were investigated by recording UV-melting curves. Generally, when DNA undergoes ligand-induced condensation, it can have a different melting profile compared to that of free DNA. In Figure 3A, the melting of free GC-DNA resulted in a sigmoidal curve with a T_m value of 64 °C. In the presence of 1 mM spermine, the melting curve of GC-DNA showed complex behavior with the presence of more than one transition. The decrease in absorbance during the first transition may be an indication of DNA undergoing significant structural alteration such as aggregation or condensation. Remarkably, when the concentration of spermine was increased to 4 mM, the downward transition disappeared and the melting curve returned to its original (sigmoidal) shape, without any change in the DNA melting stability (similar to free DNA). This process is comparable to the well-recognized DNA resolubilization by a cationic ligand.[30] Similarly, in Figure 3B, in the presence of protamine, GC-DNA gives a complex curve in which the transition in the lower temperature range is due to the alteration in DNA conformation.[6] Likewise, in the case of Ni^{2+} (Figure 3C), the melting curve of GC-DNA goes downward and then upward, suggesting that the DNA-Ni^{2+} interaction has also resulted in a significant alteration in the structure of GC-DNA.[6] Analogously, cohex shows a similar but sharper melting profile for GC-DNA as shown in Figure 3D.

Here, abnormal melting profiles registered for GC-DNA include two separate transitions; the first corresponds to the formation of a new DNA−ligand structure, and the second transition is ascribed to the destruction of that DNA system. Temperature-induced aggregates of higher-ordered assemblies are quite common for biopolymers in the presence of cations.[31] When the T_m is reached, the aggregates dissolve extensively.[32] The ability of a cation to alter the DNA structure can be

https://doi.org/10.1021/acsomega.2c01557
ACS Omega 2023, 8, 4554−4565

attributed to its ability to disrupt DNA base pairing and simultaneously cross-link with two different sites.

In Figure 3E, free AT-DNA showed a sigmoidal curve with a melting temperature (T_m) of 60 °C. In the presence of 1 mM spermine, the melting curve showed non-sigmoidal behavior similar to GC-DNA (Figure 3A), indicating an alteration in DNA conformation. In the presence of 4 mM spermine, the curve returned to its sigmoidal shape with no change in T_m. This is exactly similar to GC-DNA, suggesting the resolubilization of aggregates formed at the lower concentration of spermine.[20] Thus, spermine induces an alteration in DNA conformation, which is independent of the DNA sequence. In Figure 3F, AT-DNA in the presence of protamine gives a biphasic curve in which lower T_m (58 °C) and the higher T_m (68 °C) can be related to free and protamine-bound DNA, respectively.[33] The bound state indicates protamine-stabilizing DNA by 10 °C. On the contrary, Ni^{2+} ions did not induce a significant change in the melting temperature of the DNA, which suggests that it does not interact with AT-DNA strongly enough (Figure 3G), also supported by CD results. The post-transition drift observed in the melting curve may be due to temperature-induced aggregation of the DNA-Ni^{2+} complex at higher temperatures. Interestingly, cohex stabilizes AT-DNA, giving a biphasic transition—the first transition for free DNA and the second for the bound DNA (Figure 3H).

UV–vis Absorbance Spectra. The change in DNA absorbance at 260 nm can be used to understand the structural alteration in DNA upon ligand-binding. Upon the addition of spermine, there is a decrease in absorbance of GC-DNA and AT-DNA, indicating a loss of their DNA structure (Figure 4A)

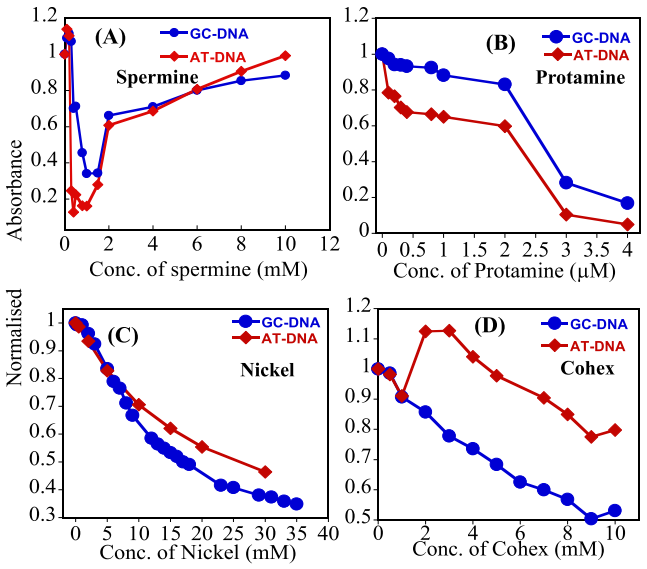

Figure 4. UV condensation measurements of GC- and AT-DNA in the presence of (A) spermine, (B) protamine, (C) Ni^{2+}, and (D) cohex. The absorbance values were recorded at 260 nm for GC- and AT-DNA. Time-dependent measurements of DNA condensates using UV–vis absorption.

up to 1 μM. However, the effect is stronger in the case of AT-DNA, suggesting that AT-DNA is more susceptible to structural modifications by spermine. When the concentration of spermine was increased beyond 1 μM, absorbance started increasing again. This is in good agreement with the melting studies, where we saw the reversal of the melting transition at higher spermine concentrations. On the contrary, in the case of protamine, the decrease in absorbance happens in more than one phase for both GC- and AT-DNA. Similarly, for Ni, absorbance values decreased more rapidly for GC-DNA compared to those for AT-DNA. Interestingly, there is an increase in the absorbance when cohex is added initially to AT-DNA, indicating the stabilization of DNA (Figure 4D), which is also supported by T_m results (Figure 3H). However, further additions of cohex to GC-DNA resulted in a continuous decrease in absorbance, suggesting the aggregation of DNA.

To explore the time-dependent changes in the absorbance of the ligand–DNA complexes, we monitored their UV–vis spectra at different time intervals (Figure 5). The absorbance values for the complex of GC- and AT-DNA with 1 mM spermine were found to decrease (70% in 10 h) continuously with an increase in time, indicating a serious alteration in the structure of DNA by spermine (Figure 5A). However, in the presence of 4 mM spermine, there was no change in absorbance even after 10 h of incubation for both the DNAs (Figure 5C,D). Moreover, it was observed that in 1 mM spermine there was a broadening and splitting of the peak at a time interval of 6–10 h with the solution becoming turbid, whereas there was no such noticeable change in λ_{max} (which is similar to the naked DNA) at 4 mM concentration of spermine with the solution being transparent throughout the experiment. This confirms that DNA can retain its original conformation at a higher concentration of spermine. The results are strongly supported by the UV studies in Figures 3A,E and 4A.

In the case of protamine, there is a decrease in the absorbance as a function of time for both GC- and AT-DNA (Figure 5E,F). Since the decrease in absorbance is taking place with both the DNAs, it is difficult to suggest whether it is due to the formation of condensates or multimolecular aggregates. However, as observed in CD, protamine induces a psi type of structure in GC-DNA but not in AT-DNA. Therefore, it is reasonable to say that the decrease in absorbance in GC-DNA is due to condensation, whereas it could be due to aggregation in AT-DNA. In our earlier study also, we observed single DNA molecules collapsing into a toroidal form, as well as multiple molecules being arranged into aggregates.[6] Interestingly, there is a small time-dependent effect of Ni^{2+} on GC-DNA but no change in AT-DNA (Figure 5G,H). Furthermore, in the presence of cohex, there is a decrease in the absorbance when complexed with GC-DNA, which confirms the loss in the confirmation of DNA with time (Figure 5I). However, in the case of AT-DNA, no such change in the absorbance intensity (Figure 5J) was observed at 1 mM cohex, which would mean that it may be involved in stabilization of the DNA. The initial upward curve in Figure 4D observed for AT-DNA supports this, which is also further backed by the melting study (Figure 3H).

Gel Electrophoresis. To support the above results, we also performed the select gel electrophoresis experiments at various P/D bp^{-1} ratios (Figure S1) for GC-DNA in the presence and absence of Ni, spermine, protamine, and cohex. Here, the band intensities can be compared for free versus ligand-bound GC-DNA. We observed that, with the increase in the ligand concentration (for all the ligands), there is a loss of band intensity, which is an indication that DNA is undergoing topological changes such as condensation.[6] These results support the analysis from CD and UV–vis studies (Figures 2–4).

https://doi.org/10.1021/acsomega.2c01557
ACS Omega 2023, 8, 4554–4565

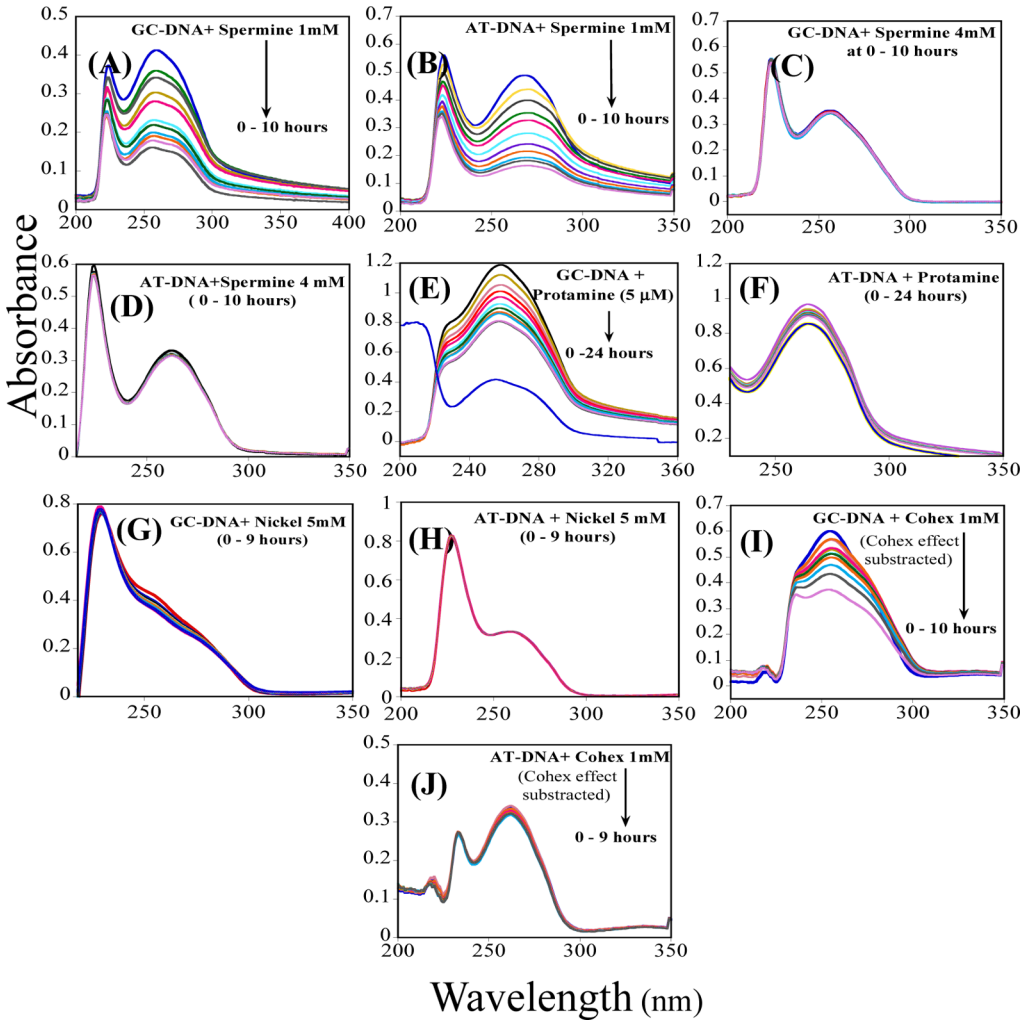

Figure 5. Time-dependent absorption spectral changes for (A) GC-DNA with 1 mM spermine, (B) AT-DNA with 1 mM spermine, (C) GC-DNA with 4 mM spermine, (D) AT-DNA with 4 mM spermine, (E) GC-DNA with 5 μM protamine, (F) AT-DNA with 5 μM protamine, (G) GC-DNA with 5 mM Ni^{2+}, (H) AT-DNA with 5 mM Ni^{2+}, (I) GC-DNA with 1 mM cohex, and (J) AT-DNA with 1 mM cohex.

Binding Thermodynamics of the DNA−Ligand Interaction. Figure 6 shows ITC-binding isotherms of various ligands with AT- and GC-DNA. The binding of the spermine was found to be slightly biphasic, which was fitted using the two-site binding model. The binding to AT (K_{A1} = [(1.0 ± 0.26) × 10^6 M^{-1}] was slightly higher compared to GC-DNA (K_{A1} = [(1.0 ± 0.15) × 10^5 M^{-1}] as shown in Figure 5A,E.[28] The K_{A2} values for second sites are relatively low, indicative of weak non-specific interactions. The ability of spermine to bind the AT as well as the GC sequence suggests an important role of non-specific interaction in binding. The binding is enthalpically unfavorable and entropically favorable in both cases (Table 1). The entropically favorable interaction supports the role of electrostatic interaction and solvation entropy in the binding.[6] The electrostatic binding has resulted in the charge neutralization responsible for condensation. The *N* value (0.2 and 0.3) suggests one spermine binding per 3−5 bp of DNA. Similarly, the binding between protamine and GC-DNA is entropically dominant with a binding constant of [K_A = (3.2 ± 0.3) × 10^5 M^{-1}], whereas no measurable binding (scattered data) was observed in the case of AT-DNA (6B and 6F).

Ni showed a higher binding affinity for GC-DNA [(2.3 ± 0.7) × 10^5 M^{-1}] than AT-DNA [(5.4 ± 0.4) × 10^4 M^{-1}] (Figure 6C,G; Table 1). The *N* value (0.8) suggests nearly one Ni binding per one DNA bp. The reaction is dominated by favorable entropy terms in both cases (ΔS = +6.2 and +5.8 kcal mol^{-1}, respectively), suggesting the role of solvation entropy in binding.[34] When binding was performed at variable salt concentrations, it was observed that the affinity of Ni^{2+} to GC-DNA decreased with an increase in salt concentration from [(2.3 ± 0.7) × 10^5] M^{-1} at 10 mM salt (Figure 6C) to [(5.4 ± 0.6) × 10^4] M^{-1} at 25 mM salt (Figure S1A and Table S1). However, in the case of AT-DNA, the binding at higher salt (Figure S1B) was completely abolished, suggesting that AT-Ni complexation is dominated by a weak non-specific interaction. This indicates that the Ni−GC complex formation is driven by specific interactions, which is also supported by a higher negative enthalpy change (−1.11 kcal/mol^{-1}). Thus, the strength of the binding in the Ni^{2+}-DNA interaction is intensely reliant upon the base composition of the DNA.

In Figure 6D, the ITC titration curve indicates that cohex binds to GC-DNA in two stages; in the first stage, it binds to neutralize a certain fraction of the negative charge on the DNA [K = (1.5 ± 0.7) × 10^5] M^{-1}; ΔH = 1.0 ± 0.3 kcal mol^{-1}; $T\Delta S$ = 8.1 ± 1.5 kcal mol^{-1}]. Thereafter, further additions of cohex result in the neutralization of the additional negative charge on the DNA with the evolution of the second transition (K = (1.0

https://doi.org/10.1021/acsomega.2c01557
ACS Omega 2023, 8, 4554−4565

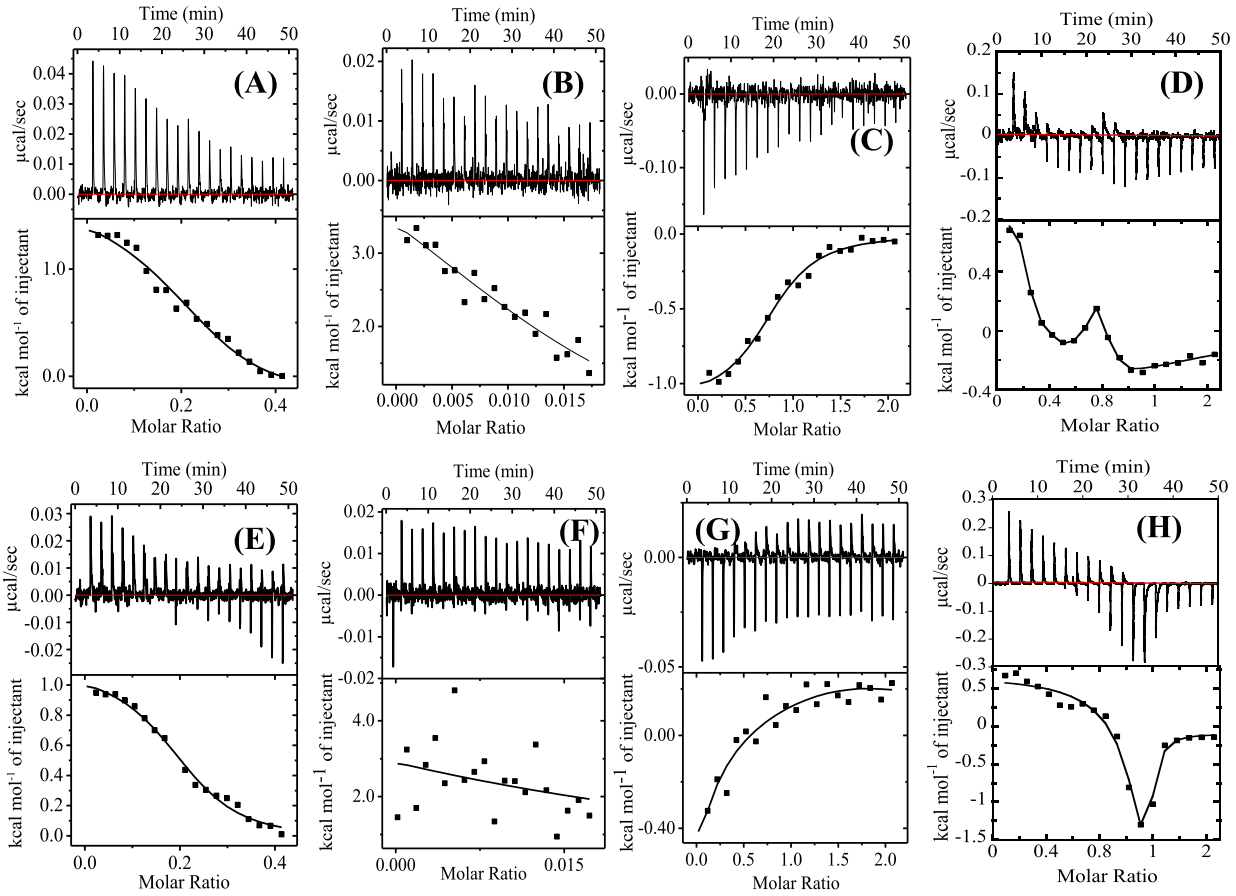

Figure 6. ITC-binding thermograms of GC-DNA with (A) spermine, (B) protamine, (C) Ni, and (D) cohex; and AT-DNA with € spermine, (F) protamine, (G) Ni, and (H) cohex. The upper panel signifies the data for the successive injection of the ligand into DNA, and the bottom panel displays the integrated heat after correction of heat due to buffer.

$\pm$ 0.5) $\times$ 10^7 M^{-1}; ΔH = 0.5 $\pm$ 0.1 kcal mol^{-1}; $T\Delta S$ = 10.1 $\pm$ 1.9 kcal mol^{-1}), which can be assigned to DNA condensation and aggregation.[8] Similar behavior was reported earlier for the interaction of the cationic lipid with DNA.[13] AT-DNA (Figure 6H) also shows a biphasic curve in which the first stage is a result of ligand binding to DNA driven by endothermic heat and positive entropy (K = (2.1 $\pm$ 0.9) $\times$ 10^4 M^{-1}; ΔH = 1.3 $\pm$ 0.4 kcal mol^{-1}; $T\Delta S$ = 7.2 $\pm$ 1.5 kcal mol^{-1}). The curve in the second stage (K= (3.0 $\pm$ 0.7) $\times$ 10^6 M^{-1}; ΔH = $-$1.6 $\pm$ 0.3 kcal mol^{-1}; $T\Delta S$ = 7.2 $\pm$ 1.5 kcal mol^{-1}) is much deeper with the involvement of exothermic heat, which could be an indication of the formation of aggregates. We have observed similar results earlier for calf thymus DNA.[6] The N values (0.25 $\pm$ 0.1 and 0.55 $\pm$ 0.2) suggest cohex binding to 2$-$5 bp of DNA.

Fluorescence Displacement Studies Using EtBr and DAPI. To reveal the nature of ligand-binding modes that drive DNA condensation, we performed EtBr and DAPI fluorescence displacement assays. Generally, ligands recognize DNA via three general modes: intercalation, groove, and electrostatic interaction.[35] EtBr and DAPI, which are strong fluorescent dyes, are known to bind to DNA through intercalation and minor groove-binding modes, respectively.[36] Thus, when the ligand is added to the DNA$-$drug complex, a decrease in fluorescence intensity may be observed, which is an indication that the ligand is displacing the drug from its DNA site. Based on the ability of a ligand to displace DAPI or EtBr, its DNA-binding mode can be estimated.

Figure 7A shows the plot of change in emission intensity due to displacement of the drug by the ligand versus the concentration of the ligand. Here, EtBr gives a strong emission peak at 610 nm upon binding with the DNA through the intercalation mode.[6] In the case of GC-EtBr, the ability of ligands to displace EtBr follows the order: protamine > cohex > Ni > spermine (Figure 7A), and the corresponding IC_{50} values (the concentration of ligand required to displace 50% of the dye) were 1.1, 490, 905, and 4100 μM. In the case of AT-EtBr (Figure 7B), the order is protamine > spermine > cohex > Ni, and IC_{50} values are 1.4, 700, 1100, and 2100 μM, respectively (Figure 7D). Interestingly, based on the ligand order, in the case of AT-DNA, there is a good correlation between the ligand charge and its ability to displace the drug. However, in GC-DNA, there is no such correlation observed, which indicates that GC condensation is not just influenced by electrostatic interaction but ligand-specific interactions are also crucial. Amongst all the ligands, protamine displayed the strongest ability to displace drugs from both the DNAs, which may be due to its larger size and the presence of multiple Arg residues. Noticeably, six times higher spermine is required to displace EtBr from the GC- compared to AT-DNA. This shows that spermine does not compete directly with EtBr (an intercalator) for GC sites.

On the other hand, Ni displaces EtBr more efficiently from GC-DNA compared to AT-DNA, which could be due to its ability to recognize guanines with higher specificity than adenines. This is well supported by ITC, where Ni binds better

https://doi.org/10.1021/acsomega.2c01557
ACS Omega 2023, 8, 4554$-$4565

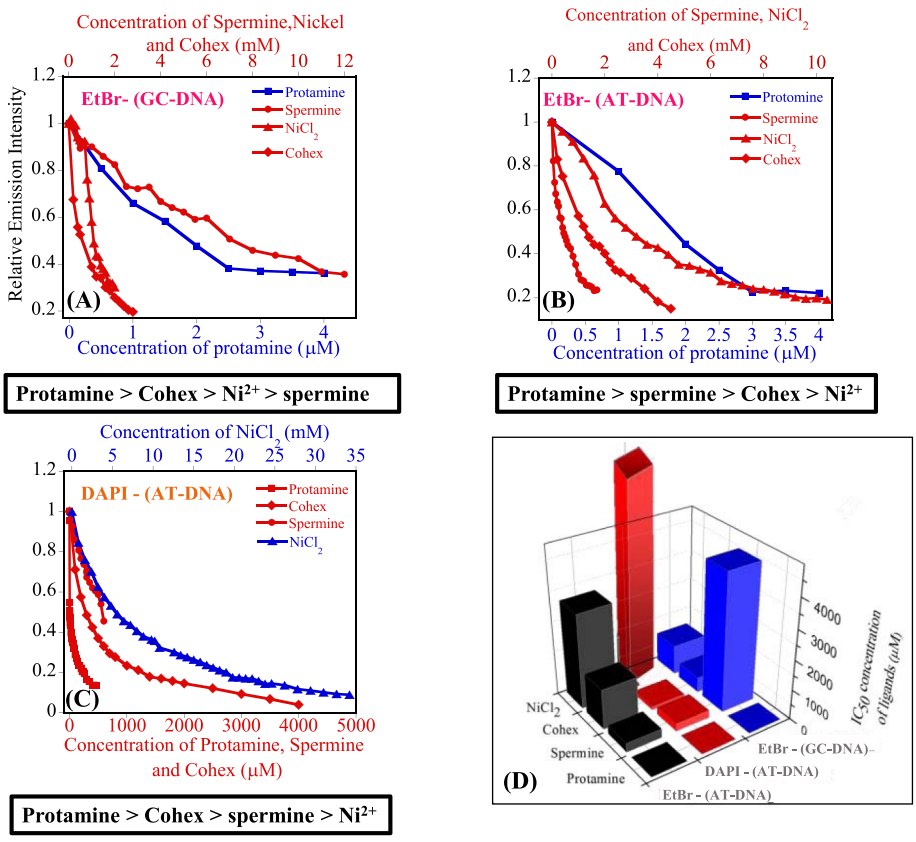

Figure 7. Fluorescent drug displacement plots of (A) EtBr-GC-DNA, (B) EtBr-AT-DNA, and (C) DAPI-AT-DNA by the binding of spermine (●), protamine (■), cohex (♦), and Ni^{2+}(▲) and (D) the comparison of the corresponding IC_{50} values using histogram plots.

to GC- than AT-DNA, and UV-melting, where Ni could induce alteration in GC-DNA. Also, Ni^{2+}, despite having fewer positive charges compared to spermine^{4+}, is much more effective in displacing EtBr from GC-DNA. This confirms the overall significance of the DNA-binding affinity and specificity of the ligand in DNA condensation. Furthermore, only half of the cohex concentration was required to displace EtBr from GC-DNA compared to AT-DNA, which could be due to its ability to bind and induce conformational changes in GC-DNA as supported by CD, ITC, and melting studies. Although cohex has one less positive charge than spermine, it is more effective in condensing GC-DNA, which could be due to its compact structure and ability to exert base-specific contacts with GC-DNA.

In Figure 7C, the displacement of DAPI from AT-DNA by all the four ligands follows the order: protamine > cohex > spermine > Ni (Figure 7D), with the corresponding IC_{50} values of 13.3, 210, 495, and 5000 μM, respectively. It was observed that the displacement of DAPI from AT-DNA requires 10 times higher protamine concentration compared to the displacement of EtBr. This is because DAPI forms a much stronger complex with AT-DNA compared to EtBr.[6] Cohex also shows a strong ability to displace DAPI from AT-DNA, indicating its ability to compete with DAPI binding sites on DNA, supported by the formation of a moderately stable AT-cohex complex in the melting study. Ni is required in very high concentrations to displace DAPI from the minor groove of AT, probably because it does not compete directly with DAPI binding sites.

DISCUSSION

Ligand-Binding Modes Play a Vital Role in DNA Condensation. Protamine is instrumental in condensing and packaging the DNA in mature human spermatozoa. It consists of 21 Arg residues with the potential to form a wide range of interactions with DNA. The extended structure of protamine and endothermic heat in ITC suggest that protamine can bind externally to the DNA backbone. As far as DNA condensation is concerned, it acts in a very sequence-specific manner and condenses only GC-specific DNA. This is based on its ability to induce the ψ structure in GC-DNA (Figure 2B), which is known to promote the bending properties of DNA and also condensation.[37] Earlier, using ctDNA, we had proposed that GC stretches in the DNA sequence are crucial for DNA condensation.[6]

Furthermore, protamine caused the stronger displacement of GC-bound EtBr compared to AT-bound EtBr, essentially through specific H-bond interactions of Arg-NH (of protamine) with G-N_7. Arg has a higher pK_a (~13.8) with a strong tendency to remain charged at physiological pH. Also, each Arg has a guanidinium group, which has the potential to promote bidendate hydrogen bonding with the phosphate oxygens and N_7 and O_6 (acceptors) of guanine in the major groove of the DNA.[38] Here, the major groove can provide more H-bonding sites on DNA than the minor groove. Earlier, Arg-rich peptides have been shown to interact in a similar fashion.[39] Also, the larger size of protamine is suitable to fit in the GC-major groove, which is also larger in size. The flexible conformation of protamine allows it to achieve the maximum possible H-bonds with DNA, which is favorable entropically also (Table 1). The minor groove, on the other hand, is too

https://doi.org/10.1021/acsomega.2c01557
ACS Omega 2023, 8, 4554−4565

narrow for protamine binding. As a result of protamine binding in the major groove, the phosphates on both strands can get attracted to the groove-bound ligand, leading to groove closure, accompanied by DNA bending toward the ligand. In the past, major groove binding associated with the bending of the DNA was suggested for GC-DNA.[40] On the contrary, the N_7 atom of adenine is known to form a weaker interaction with Arg compared to the N_7 atom of guanine.[41] Furthermore, between AT-bound EtBr and AT-bound DAPI, protamine affects easier displacement of the former (Figure 7), indicating its inability to displace DAPI. This clearly establishes that protamine has poor accessibility to the AT minor groove.

When it comes to DNA condensation, only cations with more than +3 charges are considered to be effective. Divalent metal cations do not aggravate the condensation phenomenon except at a very high concentration[42] or under distinctive conditions, such as in water-alcohol mixtures.[43] It is generally considered that cations bound even at the most favorable sites on B-form DNA readily exchange with the solution, and they are not considered as strongly bound by any criteria. Nevertheless, the preferential localization of cations at some sequences over others implies their DNA sequence-dependent binding.[44] Previously, Ni^{2+} showed a successful condensation of DNA;[21] however, the study reported mostly qualitative analysis. Here, we have concluded that Ni can induce condensation specifically in GC-DNA based on the following experimental outputs: (i) Ni has about five times better affinity for GC- compared to AT-DNA; (ii) Ni is much more effective in displacing GC-bound EtBr compared to AT-bound EtBr, indicating its ability to recognize guanines more specifically; (iii) Ni induces a characteristic psi type of spectrum in GC-DNA; (iv) Ni induces time-dependent loss of GC at 260 nm in UV−vis, an indication of condensation of DNA; and (v) unusual melting of GC by Ni as opposed to AT, which shows normal melting. The ability of Ni^{2+} to selectively recognize the N_7 atom of the guanine[45] imitates its site-specific binding to the DNA containing GC base pairs. Similar observations were made earlier, where authors have revealed that the extent of binding between AMP/GMP and Ni is mainly driven by the basicity of N_7.[46] Recently, it has also been observed that Ni binds G-C in the double helix from the side of the major groove, thus forming bridges between G-N_7 of one chain and G-N_7 of the opposite chain (Vasil et al. arXiv open-access repository). The stoichiometry ($N \sim 1.0$) suggests one Ni binding per single bp. The N_7 positions are well accessible in the major groove of duplex DNA. This leads to the binding of multiple Ni to DNA, leading to the partial charge neutralization of DNA strands and their condensation.[47]

To dig deeper into the mechanism, we performed an EtBr displacement assay on two nickel-bound GC-containing sequences, seq1 (with GC at the terminal ends d-$(CGTATATACG)_2$) and seq2 (with GC in mixed positions [$d(CGTGTACACG)_2$). The difference in the number and position of GC bases allows detecting the accessibility of GC bases to Ni. The sequences were selected based on an earlier X-ray study[45] (PDB ID: 1G3V). In the fluorescence binding study (Figure 8A), EtBr binds better to seq2 (containing more GC bases) than to seq1. However, in the EtBr displacement study (Figure 8B), Ni shows equal displacement of EtBr in both the sequences observed by the decrease in fluorescence intensity upon the addition of Ni^{2+}. This suggests that Ni may be displacing EtBr only from the terminal GC base pairs, which further suggests that Ni has better access to terminal GC base pairs. Previously, Sitko et al. have shown that Ni binding has resulted in the ends of single GC-DNA molecules being folded on themselves, producing tennis racket-shaped condensates.[21] This unambiguous result gives evidence that Ni prefers binding to terminal GC, and the process, which is driven by steric accessibility, drives DNA condensation.[21] On the contrary, Ni could not easily displace AT-bound DAPI (Figure 7), which shows that it has a weaker affinity for the AT sequence (supported also by T_m). This gets support from crystal data, where Ni can associate with N_7 atoms of all the guanines but not with adenines.[22]

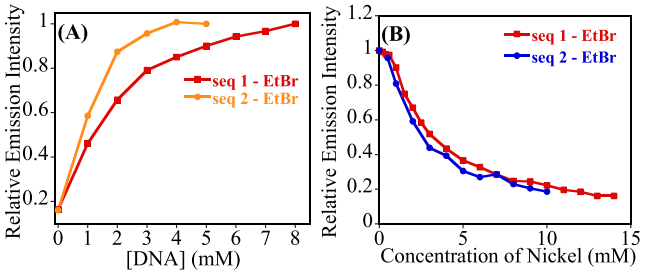

Figure 8. Fluorescence study (A) binding plot of EtBr with seq1 and seq2; (B) displacement of EtBr by Ni from the EtBr complex with seq1 and seq2.

The nature of the DNA−spermine complex has received considerable attention.[19,48,49] In the past, Feuerstein et al.[40] found that spermine shows a preference for the major groove of B-DNA, followed by a minor groove, with some binding to the phosphate groups. However, which one of these modes would be dominant in DNA condensation is still unresolved. Based on results here, spermine induces complete condensation in GC-DNA and faces resistance in AT-DNA. Here, the use of the pure AT versus GC sequence gives an opportunity to shed more light on the spermine's probable binding mode in DNA condensation. Based on the ITC results, spermine is likely to bind in the minor groove of AT-DNA[48] because the minor groove of the AT sequence is deep and narrow, which is better suited for spermine binding. This is further supported by stronger displacement of DAPI (compared to EtBr) by spermine from the AT sequence. However, deeper minor grooves may promote the internalization of bound spermine molecules rather than exposing them to neighboring helices for DNA−DNA attraction. Thus, groove geometry may play a vital role in the resistance of AT-DNA to condensation by spermine.

However, the ability of spermine to bind equally well to GC in ITC suggests that spermine may be occupying the major groove of the GC-DNA because its binding in the minor groove is prohibited due to steric hindrance from the G-NH_2 group.[50] Recently, MD analysis found that spermine remained bound to the major grooves of the respective DNA molecules for the entire simulation duration.[51] Here, GC-DNA is expected to undergo condensation by spermine as bending in the major groove would favor condensation, as also reported earlier.[40] From the FDA results, successful EtBr displacement by spermine from GC-DNA does not rule out a secondary role of electrostatic interaction between spermine's cationic ends and phosphate backbone in DNA condensation.

ITC studies revealed that cohex binds to both GC- and AT-rich sequences; however, the observed biphasic curve is more pronounced in GC, suggesting that the condensation phenomenon is more intense in the GC-rich sequence. This

https://doi.org/10.1021/acsomega.2c01557
ACS Omega 2023, 8, 4554−4565

is also supported by the unusual melting transition of GC observed in the presence of cohex. Also, the fact that cohex is more effective in displacing GC-bound EtBr compared to AT-bound EtBr in FDA indicates its ability to induce marked conformational changes in GC. Furthermore, the decrease in the 260 nm peak in UV suggested the loss of the B-form of GC-DNA by cohex, whereas no such change was observed for AT-DNA. These results confirmed the ability of cohex to act on DNA in a sequence-specific manner. Here, multiple modes of binding by cohex may drive GC-DNA condensation. In ITC, the positive entropies overcome small enthalpies, indicating that the interactions are entropically driven. Generally, such an effect is due to the charge−charge interaction, which is often accompanied by the loss of counterions and the disruption of the hydration layer, driven by favorable entropy and unfavorable enthalpy. The stoichiometry value in ITC suggests that a single cohex covers almost four base pairs in the GC-DNA binding. Since a minor groove of GC is blocked by the G-NH_2 group, here, cohex can occupy the major groove of GC-DNA. In GC-DNA, the edges of the bases in the major groove present an electrostatically negative face, and since cohex is cationic in nature, electrostatic binding supports the initial driving force for its affinity to GC-DNA, which is also favored by higher endothermic ΔH and positive entropy (Table 1). Furthermore, a greater preference of cohex for the N_7 atom of guanine[52,53] can certainly strengthen these interactions. Previously, such binding of cohex in the major groove of RNA was reported through hydrogen bonding with the N_7 and O_6 of guanine residues.[54]

CONCLUSIONS

In this paper, we studied, using diverse biophysical means, the DNA-condensing abilities and the corresponding binding modes of four ligands. An interesting picture emerged of the sequence specificity of DNA condensation by these ligands in which the phenomenon is driven by major structural alterations in the DNA. Protamine, which has a larger size and a greater number of positive charges, has the strongest ability to selectively alter the GC-DNA structure and thereby induce its condensation. Interestingly, Ni^{2+} is shown to be more efficient in condensing GC-DNA (but not AT-DNA) compared to spermine^{4+}. Spermine induces conformational alteration in GC as well as AT-DNA; however, it induces condensation in GC-DNA only. Interestingly, cohex induces conformational alteration in AT-DNA while condensation in GC-DNA. In general, GC-DNA sequences are extremely flexible to experience transition from the B- to psi type of DNA, which facilitates the condensation. Furthermore, the major groove binding by ligands seems to be the favorable mode of interaction during GC-DNA condensation. The low concentration of protamine required to induce DNA condensation compared to other ligands indicates that molecules having a larger size with chained multiple cationic charges will have an advantage in forcing the DNA toward condensation. On the other hand, smaller cations are too disorganized in solution to have a collaborative effect, and they may be required in very high concentrations to induce DNA condensation.

ASSOCIATED CONTENT

Supporting Information

The Supporting Information is available free of charge at https://pubs.acs.org/doi/10.1021/acsomega.2c01557.

Gel electrophoresis study; ITC-binding studies of Ni^{2+} with GC- and AT-DNA at 25 mM salt; and table for parameters for the interaction of Ni^{2+} with GC- and AT-DNA at 25 mM NaCl concentrations (PDF)

AUTHOR INFORMATION

Corresponding Author

Manoj Munde − *School of Physical Sciences, Jawaharlal Nehru University, New Delhi 110067, India;* orcid.org/0000-0001-7724-1185; Email: mundemanoj@gmail.com

Authors

Sakshi Gupta − *School of Physical Sciences, Jawaharlal Nehru University, New Delhi 110067, India; Department of Applied Science, The NorthCap University, Gurgaon, Haryana 122017, India*

Soumya Aggarwal − *School of Physical Sciences, Jawaharlal Nehru University, New Delhi 110067, India*

Complete contact information is available at: https://pubs.acs.org/10.1021/acsomega.2c01557

Author Contributions

The manuscript was written through contributions of all authors. All authors have given approval to the final version of the manuscript.

Notes

The authors declare no competing financial interest.

ACKNOWLEDGMENTS

This work was supported by grants from DST SERB (ECR/2016/000942), DST DPRP (P/569/2016-1/TDT), DST-IRHPA (IPA/2020/000007), UPEII JNU, and DST Purse. We also thank AIRF for instrument facility.

REFERENCES

(1) Boettiger, A. N.; Bintu, B.; Moffitt, J. R.; et al. Super-resolution imaging reveals distinct chromatin folding for different epigenetic states. *Nature* **2016**, *529*, 418−422.

(2) Carrivain, P.; Cournac, A.; Lavelle, C.; et al. Electrostatics of DNA compaction in viruses, bacteria and eukaryotes: functional insights and evolutionary perspective. *Soft Matter* **2012**, *8*, 9285−9301.

(3) Bloomfield, V. A. DNA condensation by multivalent cations. *Biopolymers* **1997**, *44*, 269−282.

(4) Wilson, R. W.; Bloomfield, V. A. Counterion-induced condensation of deoxyribonucleic acid. A light-scattering study. *Biochemistry* **1979**, *18*, 2192−2196.

(5) Bloomfield, V. A. DNA condensation. *Curr. Opin. Struct. Biol.* **1996**, *6*, 334−341.

(6) Gupta, S.; Tiwari, N.; Munde, M. A Comprehensive Biophysical Analysis of the Effect of DNA Binding Drugs on Protamine-induced DNA Condensation. *Sci. Rep.* **2019**, *9*, 5891.

(7) Li, C.; Ma, C.; Xu, P.; et al. Effective and reversible DNA condensation induced by a simple cyclic/rigid polyamine containing carbonyl moiety. *J. Phys. Chem. B* **2013**, *117*, 7857−7867.

(8) Matulis, D.; Rouzina, I.; Bloomfield, V. A. Thermodynamics of DNA binding and condensation: isothermal titration calorimetry and electrostatic mechanism. *J. Mol. Biol.* **2000**, *296*, 1053−1063.

(9) Kabir, A.; Suresh Kumar, G. Binding of the biogenic polyamines to deoxyribonucleic acids of varying base composition: base specificity and the associated energetics of the interaction. *PLoS One* **2013**, *8*, No. e70510.

(10) Matulis, D.; Rouzina, I.; Bloomfield, V. A. Thermodynamics of Cationic Lipid Binding to DNA and DNA Condensation: Roles of

https://doi.org/10.1021/acsomega.2c01557
ACS Omega 2023, 8, 4554−4565

Electrostatics and Hydrophobicity. *J. Am. Chem. Soc.* **2002**, *124*, 7331−7342.
(11) Fan, Y.; Wang, H.; He, C.; Qiao, F.; Wang, S.; Wang, Y. DNA Condensation Induced by a Star-Shaped Hexameric Cationic Surfactant. *ACS Appl. Mater. Interfaces* **2017**, *9*, 23333−23341.
(12) Smith, R. J.; Beck, R. W.; Prevette, L. E. Impact of molecular weight and degree of conjugation on the thermodynamics of DNA complexation and stability of polyethylenimine-graft-poly(ethylene glycol) copolymers. *Biophys. Chem.* **2015**, *203*−*204*, 12−21.
(13) Spink, C. H.; Chaires, J. B. Thermodynamics of the Binding of a Cationic Lipid to DNA. *J. Am. Chem. Soc.* **1997**, *119*, 10920−10928.
(14) Mintzer, M. A.; Simanek, E. E. Nonviral Vectors for Gene Delivery. *Chem. Rev.* **2009**, *109*, 259−302.
(15) Estévez-Torres, A.; Damien, B. DNA compaction: fundamental and applications. *Soft Matter* **2011**, *7*, 6746−6756.
(16) Arslantas, A.; DK, A.; Hacali, N. The Interaction of Sheep Genomic DNA with a Cobalt(II) Complex Containing p-Nitrobenzoate and N,N' Diethylnicotinamide Ligands. *Int. J. Mol. Sci.* **2007**, *8*, 1225−1233.
(17) Maffeo, C.; Yoo, J.; Comer, J.; Wells, D. B.; Luan, B.; Aksimentiev, A. Close encounters with DNA. *J. Phys. Condens. Matter* **2014**, *26*, 413101.
(18) Champroux, A.; Torres-Carreira, J.; Gharagozloo, P.; Drevet, J. R.; Kocer, A. Mammalian sperm nuclear organization: resiliencies and vulnerabilities. *Basic Clin. Androl.* **2016**, *26*, 17.
(19) Jain, S.; Zon, G.; Sundaralingam, M. Base only binding of spermine in the deep groove of the A-DNA octamer d-(GTGTACAC). *Biochemistry* **1989**, *28*, 2360−2364.
(20) Pelta, J.; Livolant, F.; Sikorav, J. L. DNA aggregation induced by polyamines and cobalthexamine. *J. Biol. Chem.* **1996**, *271*, 5656−5662.
(21) Sitko, J. C.; Mateescu, E. M.; Hansma, H. G. Sequence-dependent DNA condensation and the electrostatic zipper. *Biophys. J.* **2003**, *84*, 419−431.
(22) Abrescia, N. G.; Malinina, L.; Fernandez, L. G.; Huynh-Dinh, T.; Neidle, S.; Subirana, J. A. Structure of the oligonucleotide d(CGTATATACG) as a site-specific complex with nickel ions. *Nucleic Acids Res.* **1999**, *27*, 1593−1599.
(23) Felsenfeld, G.; Hirschman, S. Z. A neighbor-interaction analysis of the hypochromism and spectra of DNA. *J. Mol. Biol.* **1965**, *13*, 407−427.
(24) Sahoo, D.; Bhattacharya, P.; Chakravorti, S. Quest for mode of binding of 2-(4-(dimethylamino)styryl)-1-methylpyridinium iodide with calf thymus DNA. *J. Phys. Chem. B* **2010**, *114*, 2044−2050.
(25) Lin, K.; Wu, G. Isothermal Titration Calorimetry Assays to Measure Binding Affinities In Vitro. *Methods Mol. Biol.* **2019**, *1893*, 257−272.
(26) Falconer, R. J.; Penkova, A.; Jelesarov, I.; Collins, B. M. Survey of the year 2008: applications of isothermal titration calorimetry. *J. Mol. Recognit.* **2010**, *23*, 395−413.
(27) Thoppil, A. A.; Choudhary, S.; Kishore, N. Competitive binding of anticancer drugs 5-fluorouracil and cyclophosphamide with serum albumin: Calorimetric insights. *Biochim. Biophys. Acta Gen. Subj.* **2016**, *1860*, 917−929.
(28) Patel, M. M.; Anchordoquy, T. J. Ability of spermine to differentiate between DNA sequences–preferential stabilization of A-tracts. *Biophys. Chem.* **2006**, *122*, 5−15.
(29) Munde, M.; Kumar, A.; Peixoto, P.; et al. The unusual monomer recognition of guanine-containing mixed sequence DNA by a dithiophene heterocyclic diamidine. *Biochemistry* **2014**, *53*, 1218−1227.
(30) Saminathan, M.; Antony, T.; Shirahata, A.; Sigal, L. H.; Thomas, T.; Thomas, T. J. Ionic and Structural Specificity Effects of Natural and Synthetic Polyamines on the Aggregation and Resolubilization of Single-, Double-, and Triple-Stranded DNA. *Biochemistry* **1999**, *38*, 3821−3830.
(31) Cherstvy, A. G.; Kornyshev, A. A.; Leikin, S. Temperature-Dependent DNA Condensation Triggered by Rearrangement of Adsorbed Cations. *J. Phys. Chem. B* **2002**, *106*, 13362−13369.
(32) Duguid, J. G.; Bloomfield, V. A.; Benevides, J. M.; Thomas, G. J. Raman spectroscopy of DNA-metal complexes. II. The thermal denaturation of DNA in the presence of Sr2+, Ba2+, Mg2+, Ca2+, Mn2+, Co2+, Ni2+, and Cd2+. *Biophys. J.* **1995**, *69*, 2623−2641.
(33) Heinrichs, A. K.; Price, M. J. Probing the effects on the thermal stability of salmon sperm DNA in the presence of metal cations by measuring dna melting temperatures. *Adv. Biotechnol. Biochem.* **2017**, *2017*, J118 Huntingdon College, Montgomery, USA: Gavin publishers.
(34) Callies, O.; Hernández Daranas, A. Application of isothermal titration calorimetry as a tool to study natural product interactions. *Nat. Prod. Rep.* **2016**, *33*, 881−904.
(35) Chaires, J. B. Drug-DNA interactions. *Curr. Opin. Struct. Biol.* **1998**, *8*, 314−320.
(36) Kellett, A.; Molphy, Z.; Slator, C.; McKee, V.; Farrell, N. P. Molecular methods for assessment of non-covalent metallodrug-DNA interactions. *Chem. Soc. Rev.* **2019**, *48*, 971−988.
(37) Ma, C.; Sun, L.; Bloomfield, V. A. Condensation of plasmids enhanced by Z-DNA conformation of d(CG)n inserts. *Biochemistry* **1995**, *34*, 3521−3528.
(38) Harms, M. J.; Schlessman, J. L.; Sue, G. R.; García-Moreno, E. B. Arginine residues at internal positions in a protein are always charged. *Proc. Natl. Acad. Sci.* **2011**, *108*, 18954.
(39) DeRouchey, J.; Hoover, B.; Rau, D. C. A Comparison of DNA Compaction by Arginine and Lysine Peptides: A Physical Basis for Arginine Rich Protamines. *Biochemistry* **2013**, *52*, 3000−3009.
(40) Feuerstein, B. G.; Pattabiraman, N.; Marton, L. J. Molecular mechanics of the interactions of spermine with DNA: DNA bending as a result of ligand binding. *Nucleic Acids Res.* **1990**, *18*, 1271−1282.
(41) Deng, H.; Bloomfield, V. A.; Benevides, J. M.; Thomas, G. J., Jr Structural basis of polyamine-DNA recognition: spermidine and spermine interactions with genomic B-DNAs of different GC content probed by Raman spectroscopy. *Nucleic Acids Res.* **2000**, *28*, 3379−3385.
(42) Nayak, A. K.; Mishra, A.; Jena, B. S.; Mishra, B. K.; Subudhi, U. Lanthanum induced B-to-Z transition in self-assembled Y-shaped branched DNA structure. *Sci. Rep.* **2016**, *6*, 26855.
(43) Votavová, H.; Kucerová, D.; Felsberg, J.; Sponar, J. Changes in conformation, stability and condensation of DNA by univalent and divalent cations in methanol-water mixtures. *J. Biomol. Struct. Dyn.* **1986**, *4*, 477−489.
(44) Rouzina, I.; Bloomfield, V. A. DNA bending by small, mobile multivalent cations. *Biophys. J.* **1998**, *74*, 3152−3164.
(45) Abrescia, N. A.; Huynh-Dinh, T.; Subirana, J. A. Nickel-guanine interactions in DNA: crystal structure of nickel-d[CGTGTACACG]2. *J. Biol. Inorg Chem.* **2002**, *7*, 195−199.
(46) Sigel, H.; Massoud, S. S.; Corfu, N. A. Comparison of the Extent of Macrochelate Formation in Complexes of Divalent Metal Ions with Guanosine (GMP2-), Inosine (IMP2-), and Adenosine 5'-Monophosphate (AMP2-). The Crucial Role of N-7 Basicity in Metal Ion-Nucleic Base Recognition. *J. Am. Chem. Soc.* **1994**, *116*, 2958−2971.
(47) Spingler, B. Anions or cations: who is in charge of inhibiting the nickel(II) promoted B- to Z-DNA transition? *Inorg. Chem.* **2005**, *44*, 831−833.
(48) Korolev, N.; Lyubartsev, A. P.; Nordenskiöld, L.; Laaksonen, A. Spermine: an ″invisible″ component in the crystals of B-DNA. A grand canonical Monte Carlo and molecular dynamics simulation study. *J. Mol. Biol.* **2001**, *308*, 907−917.
(49) Korolev, N.; Lyubartsev, A. P.; Laaksonen, A.; Nordenskiöld, L. On the competition between water, sodium ions, and spermine in binding to DNA: a molecular dynamics computer simulation study. *Biophys. J.* **2002**, *82*, 2860−2875.
(50) Kopka, M. L.; Goodsell, D. S.; Han, G. W.; Chiu, T. K.; Lown, J. W.; Dickerson, R. E. Defining GC-specificity in the minor groove: side-by-side binding of the di-imidazole lexitropsin to C-A-T-G-G-C-C-A-T-G. *Structure* **1997**, *5*, 1033−1046.
(51) Fowler, D. K.; Williams, C.; Gerritsen, A. T.; Washbourne, P. Improved knockdown from artificial microRNAs in an enhanced miR-

https://doi.org/10.1021/acsomega.2c01557
ACS Omega 2023, 8, 4554−4565

155 backbone: a designer's guide to potent multi-target RNAi. *Nucleic Acids Res.* **2016**, *44*, No. e48.
(52) Deng, H.; Bloomfield, V. A. Structural effects of cobalt-amine compounds on DNA condensation. *Biophys. J.* **1999**, *77*, 1556−1561.
(53) Thiyagarajan, S.; Rajan, S. S.; Gautham, N. Cobalt hexammine induced tautomeric shift in Z-DNA: the structure of d(CGCGCA)*d-(TGCGCG) in two crystal forms. *Nucleic Acids Res.* **2004**, *32*, 5945−5953.
(54) Kieft, J. S.; Tinoco, I. Solution structure of a metal-binding site in the major groove of RNA complexed with cobalt (III) hexammine. *Structure* **1997**, *5*, 713−721.

https://doi.org/10.1021/acsomega.2c01557
ACS Omega 2023, 8, 4554−4565